Desalination and Water Treatment
www.deswater.com
doi: 10.1080/19443994.2015.1069222

57 (2016) 14908–14918
July

Taylor & Francis
Taylor & Francis Group

Study on the fabrication and properties of FEP/SiO_2 hybrid flat-sheet membrane and its application in VMD

Kaikai Chen, Changfa Xiao, Qinglin Huang*, Chaoxin Zhang, Yanjie Wu, Hailiang Liu, Zhen Liu

State Key Laboratory of Separation Membranes and Membrane Processes, Department of Material Science and Engineering, Tianjin Polytechnic University, No. 399 West Binshui Road, Xi Qing District, Tianjin 300387, P.R. China, Tel. +86 15122705582; email: kaikchen@163.com (K. Chen), Tel. +86 22 83955934; email: 846216569@qq.com (C. Xiao), Tel. +86 22 83955794; email: huangqinglin@tjpu.edu.cn (Q. Huang), Tel. +86 15922060753; email: 1101227501@qq.com (C. Zhang), Tel. +86 15122363172; email: 191066582@qq.com (Y. Wu), Tel. +86 13821045242; email: 545968120@qq.com (H. Liu), Tel. +86 22 83955795; email: 894662732@qq.com (Z. Liu)

Received 8 December 2014; Accepted 29 June 2015

ABSTRACT

Due to the chemical structure of the perfluoro group, perfluoro-polymers, such as polytetrafluoroethylene and poly(tetrafluoroethylene-co-hexafluoropropylene) (FEP) deserves excellent properties of outstanding thermal and chemical resistance and strong hydrophobicity. In this study, FEP hybrid flat-sheet membranes were fabricated by the melt-compressed membrane formation system, which composed of FEP, micro-scale SiO_2, and Dioctyl-Phthalate (DOP). Effects of DOP and SiO_2 contents on the membrane morphologies and properties were investigated, respectively. The membranes' corresponding microfiltration performances were characterized in terms of pure water flux, mechanical strength, membrane porosity, and vacuum membrane distillation (VMD). Results illustrated that the obtained FEP flat-sheet membranes displayed a typical asymmetric structure. There were obvious enhancement of membrane's pure water flux and porosity with increasing DOP and SiO_2 contents. The salt rejections achieved as high as 99.9% by VMD process.

Keywords: Poly(tetrafluoroethylene-co-hexafluoropropylene) (FEP); Hybrid; Flat-sheet membranes; SiO_2; Properties

1. Introduction

Nowadays, membrane technology applied in various fields such as wastewater treatment [1], food processing [2], desalination [3], and many other separations become more and more popular. Especially in recent years, it is widely realized that water shortage is becoming a very serious problem [4], and using membrane technology is an energy saving and highly efficient way to treat wastewater [5]. Membrane distillation (MD) is a membrane-based water treatment process, where the driving force is a vapor pressure difference across the hydrophobic membrane [6–8]. Two essential factors of the membrane are strong hydrophobicity and proper pore size.

Polytetrafluoroethylene (PTFE) has highly symmetrical perfluoro structure [9,10], and the fluorine atoms surround the carbon backbone, yielding PTFE

*Corresponding author.

with outstanding thermal and chemical stability, strong hydrophobicity, high mechanical strength, and low coefficient of friction [11–14]. However, the commercial PTFE flat-sheet membranes are mainly manufactured by biaxial stretching technology, which suffered from inferior performance due to the poor pore structure controllability and inferior membrane formability [15]. Poly(tetrafluoroethylene-co-hexafluoropropylene) (FEP) is a random copolymer of tetrafluoroethylene (TFE) and hexafluoropropylene (HFP) including about 15 wt% HFP [16]. As same as PTFE, FEP maintains the excellent combination of thermal and chemical resistance, strong hydrophobicity, etc. [17,18].

Several previous attempts of fabricating FEP membranes can be found in the patent literatures. Parekh et al. [19] prepared FEP porous membrane from a melt blend of FEP and a chlorotrifluoroethylene (CTFE) oligomer solvent. However, this method is not desirable for the industrial fabrication of FEP membranes, since the fabrication technique does not provide good control of the membrane morphology, and the CTFE oligomer is too expensive. Covitch [20] disclosed FEP membrane formation from a solvated or partially solvated FEP/solvent mixture, which based on thermal phase separation method. However, there was no morphology or permeability data of the porous membrane structures. In our previous research [17], we had successfully spun FEP hollow fiber membrane by melt spinning method, the results showed that the FEP hollow fiber membrane was a kind of homogeneous membrane, with favorable morphology and good permeability.

In this study, the melt-compressed membrane formation system which composed of FEP, microscale SiO_2 and Dioctyl-Phthalate (DOP) were used to fabricate FEP/SiO_2 hybrid flat-sheet membrane. The morphology and permeability of the hybrid membranes were investigated.

2. Experimental

2.1. Plate vulcanization machine

The parameters of the plate vulcanization machine were tabulated in Table 1.

2.2. Materials

FEP resins (6,100, DuPont Co., Ltd.) is a commercial product and dioctyl phthalate (DOP, > 99.5%) were purchased from Tianjin Kermel Chemical Reagent Co., Ltd., SiO_2 particles with average size of 10 μm were provided by Zibo Haina Gaoke Materials Co., Ltd.

2.3. Membrane preparation

Before use, FEP resins and SiO_2 particles were dried for 12 h at 100 ± 2℃ in a vacuum oven (2 mbar) to remove moisture. Then, at a particular mass ratio, FEP, SiO_2, and DOP were homogeneously mixed under high-speed agitation. Four different mass ratios of SiO_2 particles (2, 4, 6, and 8%) were used. The mixture was placed on a stainless steel mold. Then the temperature between the molds was heated to 270℃, and the pressure between the mold was added to 40 MPa. After 10 min, the mold containing the flat-sheet membrane was quenched to room temperature by circulating water system (25℃). Finally, FEP hybrid flat-sheet membranes were obtained after DOP was extracted through immersing in ethyl ethanol for 24 h and pure water for 24 h. The plate vulcanization machine was shown in Fig. 1, while the parameters of the plate vulcanization machine were tabulated in Table 1.

2.4. Characterization

2.4.1. Differential scanning calorimetry (DSC)

The thermal properties of FEP membranes were measured by DSC (Perkin Elmer DSC-7, Germany). DSC was performed at a heating rate of 10℃ min^{-1} over the range of 0–300℃. The crystallinity value (X_c) was calculated from the following Eq. (1):

$$X_C(\%) = \frac{\triangle H}{\triangle H_m} \times 100 \quad (1)$$

where ΔH_m is the melting enthalpy for a 100% crystalline FEP (J g^{-1}), ΔH is the melting enthalpy of the mixtures measured in DSC (J g^{-1}).

Table 1
The parameters of plate vulcanization machine

Index	Parameter value	Index	Parameter value
Length (mm)	550	Compressed pressure (MPa)	40
Width (mm)	550	Pressed time (min)	10
Height (mm)	910	Temperature range (℃)	25–350
Compressed membrane size (mm)	MAX300	Temperature accuracy (℃)	±5

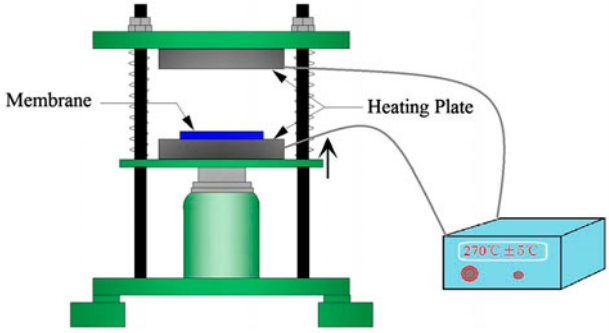

Fig. 1. Schematic of the plate vulcanization machine.

2.4.2. Porosity

The porosity was assessed by gravimetric method. Since the hydrophobicity of FEP, n-butyl alcohol was used as the wetting liquid. Eq. (2) was used to calculate ε.

$$\varepsilon(\%) = \left(1 - \frac{\rho_f}{\rho_p}\right) \times 100 \tag{2}$$

where ρ_f is membrane apparent density (kg m^{-3}, determined by a gravimetric method) and ρ_p is the polymer density (kg m^{-3}).

2.4.3. Permeability tests

The pure water flux (PWF) of the pre-wetted flat-sheet membranes was determined by the following Eq. (3), and the pressure across the membrane was 1 bar.

$$J_l = \frac{V}{A \times t} \tag{3}$$

where J_l is the PWF (L m^{-2} h^{-1}), V is the total permeation (L), A is the membrane area (m^2), and t is the sampling time (h).

Nitrogen flux of dry flat-sheet membranes was determined using a laboratory device (Fig. 2) by the following Eq. (4), and the permeate flow rate was measured at different pressure:

$$J_g = \frac{L}{A} \tag{4}$$

where J_g is the Nitrogen flux (m^3 m^{-2} h^{-1}), L is the Nitrogen flow (m^3 h^{-1}) and A is the membrane area (m^2).

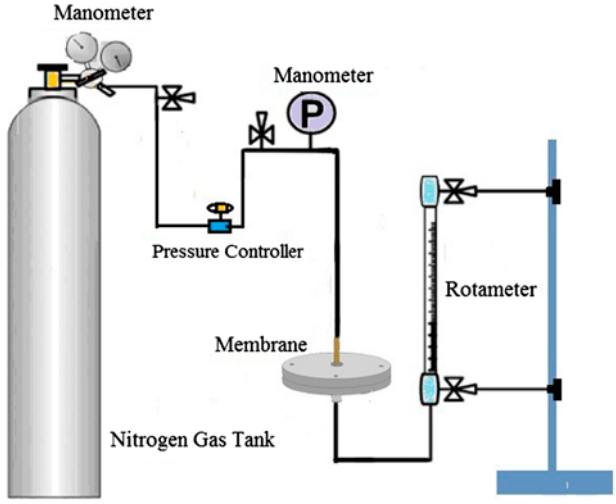

Fig. 2. Nitrogen flux of the FEP flat-sheet membrane testing device.

2.4.4. Contact angle

The contact angles of all the samples were measured by an optical contact angle meter (Jinshengxin Inspection instrument Co., Ltd., model JYSP-180). The measurements were carried out at 25℃ with 40–50% relative humidity. A water droplet was dropped on the sample surface from a distance of 5 cm by vibrating the tip of a micro syringe. The diameter of the water droplet was about 1 mm, lasting for 10 s after the droplet was dropped on the sample surface. A lens and a source light were used to create the drop image on a screen. The contact angle was determined with the projected drop image. Each sample was tested five times, and the values were averaged.

2.4.5. Liquid entrance pressure (LEP)

LEP of dry flat-sheet membranes was accessed using a laboratory device (Fig. 3) at room temperature. Increase the pressure slowly until the mutation of the conductivity meter and the value was the LEP. Each sample was tested three times, and the values were averaged.

2.4.6. Tensile break strength measurements

The tensile strength and elongation at breaking of the flat-sheet membranes were determined at room temperature using a YG-061F electronic single yarn tensile tester (Shandong, China), and the tensile rate was 2 mm min^{-1}. Five runs were performed for each specimen.

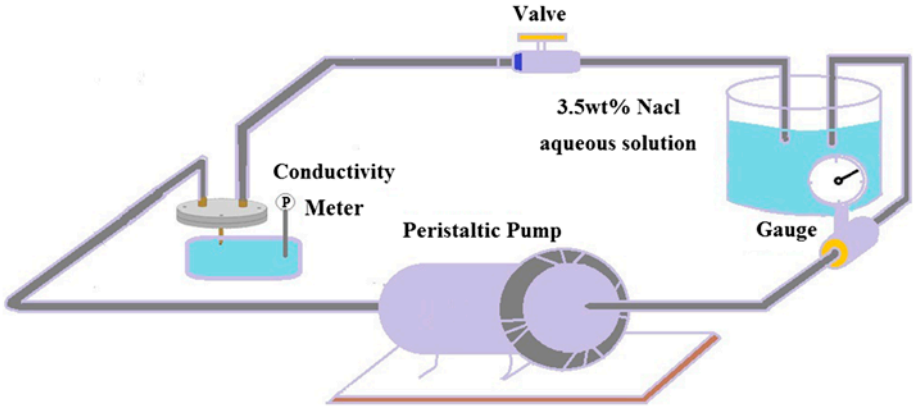

Fig. 3. LEP of the FEP flat-sheet membrane testing device.

2.4.7. Desalination experiment

Experiments of vacuum membrane distillation (VMD) were carried out to evaluate the permeate performance of flat-sheet membranes. The water desalination experiment was performed using a setup schematically shown in Fig. 4. The one side of the membrane was in contact with a hot, circulating salt solution, and the other side was connected to a vacuum pump to withdraw the permeated water vapor. The water vapor was subsequently condensed into liquid water by a glass condenser using tap water as coolant. The condensed water was collected in a glass bottle, and its volume was determined with a measuring cylinder. The conductivity of the feed solution and permeate water was measured by a conductivity meter (AP-2, HM). The NaCl rejection R was calculated by the following Eq. (5):

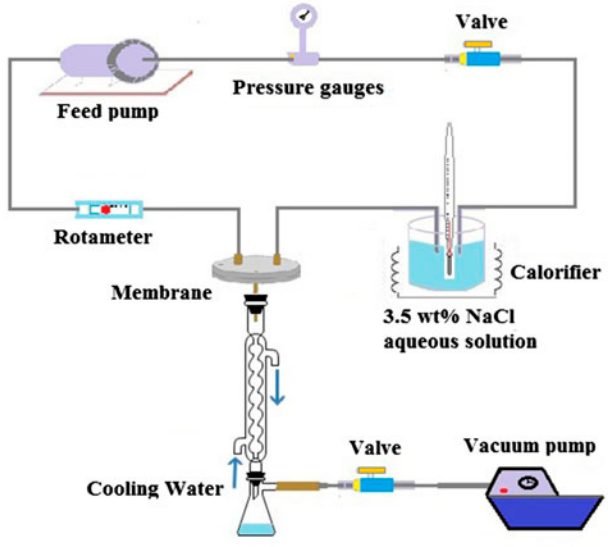

Fig. 4. Schematic diagram of the experimental VMD apparatus.

$$R = \left(1 - \frac{C_p}{C_f}\right) \times 100\% \tag{5}$$

where C_f and C_p were the conductivities of the feed solution and permeate water, respectively.

2.4.8. Morphologies observation

The morphology of the FEP flat-sheet membranes was examined using scanning electron microscopy (SEM, Nova Nano230, Netherlands FEI). Samples were frozen in liquid N_2, followed by fracturing to expose their cross-sectional areas. Thereafter, they were coated in gold and viewed by SEM.

3. Results and discussion

3.1. Thermal properties and crystallization

Effects of SiO_2 contents on the DSC curves of FEP flat-sheet membranes were shown in Fig. 5 while the data of thermal property were tabulated in Table 2. From the DSC curves (Fig. 5), it could be found that the melting peak of FEP flat-sheet membrane was observed at about 250°C. Furthermore, the melting peak moved to a higher temperature when the SiO_2 contents rose from 2 to 8 wt%. The reason could be attributed that the increased SiO_2 contents promoted the crystallization of FEP, owing to the SiO_2 particles acted as the nucleating agent, which induced a higher melting peak temperature. However, the thermal property data also showed the abnormal tendency. The melting enthalpy increased from 18 to 31.2 J g^{-1}, while the crystal temperature increased from 240.9 to

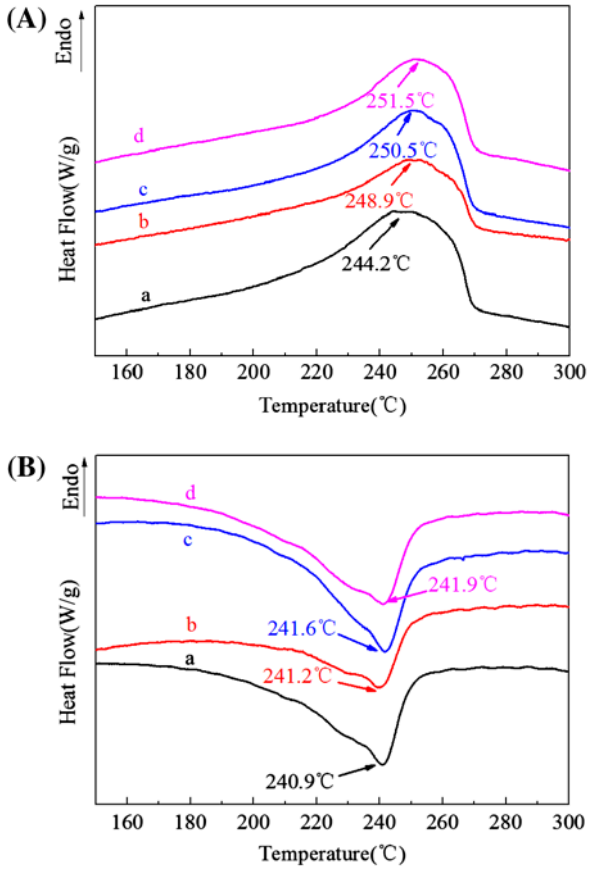

Fig. 5. DSC curves of FEP flat-sheet membranes with different SiO_2 contents, (A) heating curve and (B) cooling curve, SiO_2 contents: a-2%, b-4%, c-6%, and d-8%.

241.9℃. The reasons could be concluded that the increase in SiO_2 contents brought about a higher crystallization.

3.2. Permeation properties

3.2.1. Effect of DOP contents on porosity and permeability

Effects of DOP contents on the PWF and porosity of FEP flat-sheet membranes were shown in Fig. 6. It was clearly showed that the PWF and porosity increased with increasing DOP contents. The reasons could be concluded that the increase in the DOP contents brought about a longer coarsening time, which generated the larger pores in membrane structure. As the improvement of porosity with the increase in DOP contents which was discussed above, it was easy to understand the enhancement of N_2 flux and decrease in LEP. The effects of SiO_2 contents on the LEP and N_2 flux of the FEP flat-sheet membranes were shown in Fig. 9.

3.2.2. Effect of SiO_2 contents on porosity and permeability

The effects of SiO_2 contents on the PWF and porosity of the FEP flat-sheet membranes were shown in Fig. 8. It clearly illustrated that PWF and porosity increased with an increase in SiO_2 contents. The main reason was that interfacial microvoids (IFMs) were generated owing to the poor compatibility of FEP and SiO_2, which brought about more microvoids when the SiO_2 were dissolved in the post treatment process. As the improvement of porosity with the increase in SiO_2 contents, which were discussed above, it was easy to understand the enhancement of N_2 flux and decrease in LEP, and the results were shown in Figs. 8 and 9.

3.3. Mechanical properties

Results of the FEP flat-sheet membranes' mechanical properties were shown in Figs. 10 and 11. It could be seen that the tensile strength and elongation at breaking decreased with the increase in DOP contents. The main reason was that the increased DOP contents induced a higher membrane porosity which would weaken the tensile strength. And it could be seen that the tensile strength decreased while elongation at breaking increased with an increase in SiO_2 contents. It was well known, there is no strong affinity between FEP and SiO_2 due to the low surface energy of FEP. The increasing amount of SiO_2 would result in a reduction of mechanical strength of the FEP membranes. The results indicated that adding an appropriate amount of SiO_2 could improve the membranes' mechanical properties.

Table 2
Thermal properties of FEP flat-sheet membranes

SiO_2 contents (%)	T_m (℃)	ΔH_m (J g^{-1})	T_c (℃)	$\Delta T = T_m - T_c$ (℃)
2	242.2	18.4	240.9	1.3
4	248.9	23.1	241.2	7.7
6	250.5	24.4	241.6	8.9
8	251.5	31.2	241.9	9.6

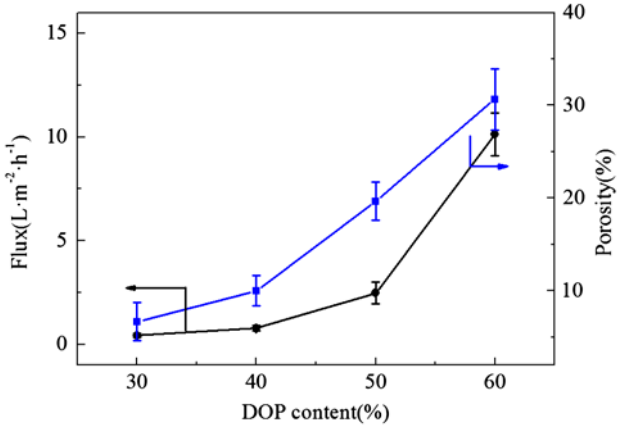

Fig. 6. Effect of the DOP contents on permeation flux and porosity.

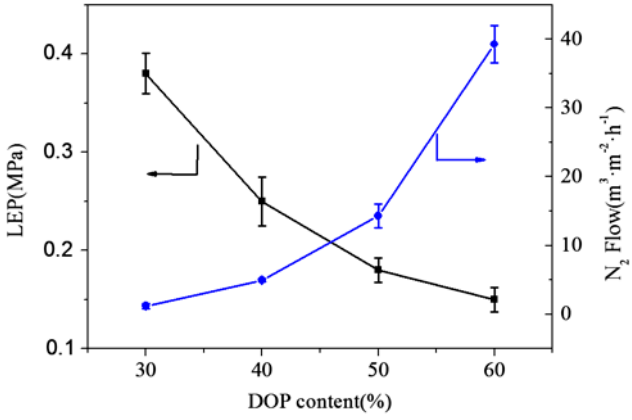

Fig. 7. Effect of DOP contents on LEP and N_2 flux.

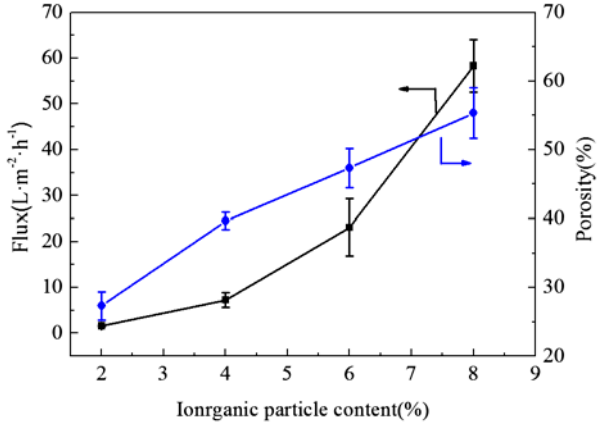

Fig. 8. Effects of the SiO_2 contents on permeation flux and porosity.

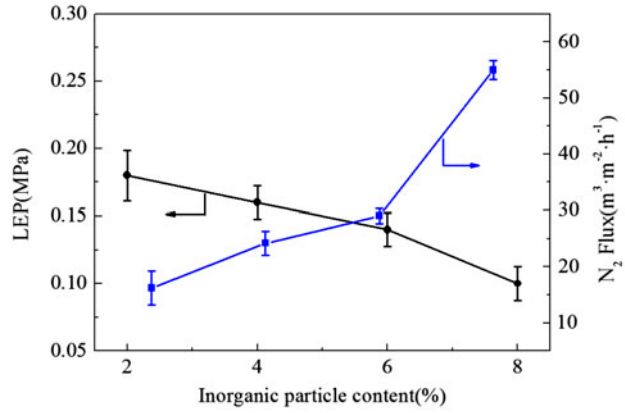

Fig. 9. Effect of the SiO_2 contents on LEP and N_2 flux.

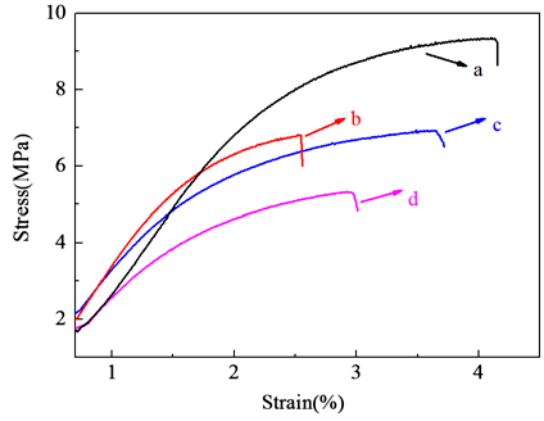

Fig. 10. Stress–strain curves of hybrid membranes with different DOP contents (a-30%, b-40%, c-50%, d-60%).

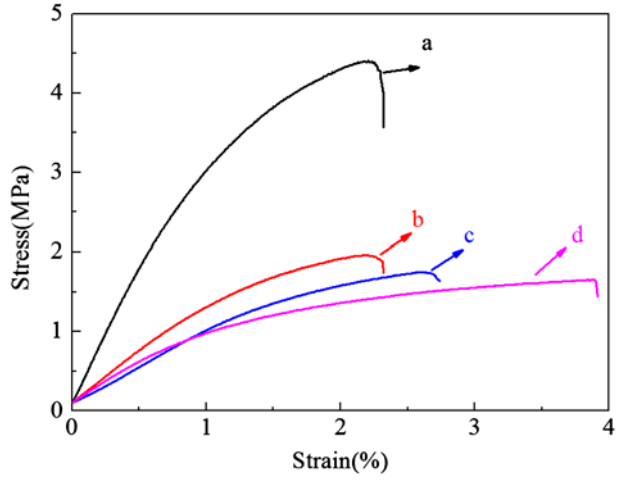

Fig. 11. Stress–strain curves of hybrid membranes with different SiO_2 contents (a-2%, b-4%, c-6%, d-8%).

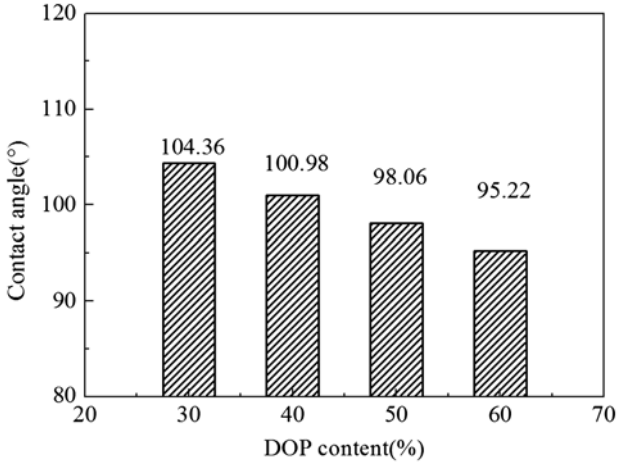

Fig. 12. Water contact angle of different DOP contents flat-sheet membranes.

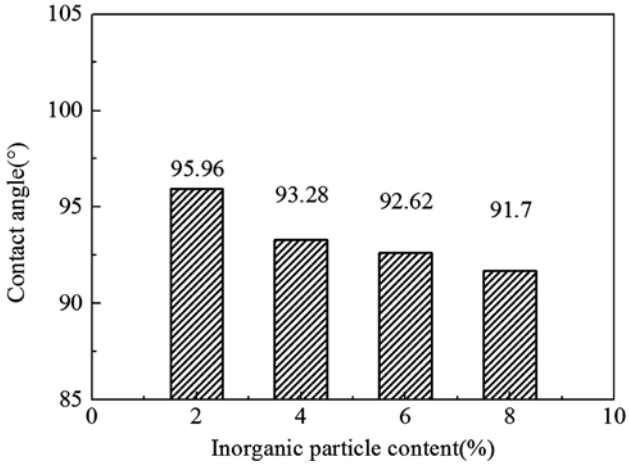

Fig. 13. Water contact angle of different SiO_2 contents flat-sheet membranes.

3.4. Membrane hydrophobicity

Hydrophobicity was the most important property for MD. The water contact angles of the FEP membranes were shown in Figs. 12 and 13. The results showed that the average water contact angle decreased from 104.36˚ to 95.22˚ as the DOP contents increased from 30 to 60 wt.%. When the SiO_2 contents increased from 2 to 8 wt%, the average water contact angle decreased from 95.96˚ to 91.70˚. The result was due to the more pore in the membrane surface, which aided the invasion of water. Moreover, SiO_2 has hydrophilic nature, so the increasing SiO_2 contents lead to more hydrophilicity.

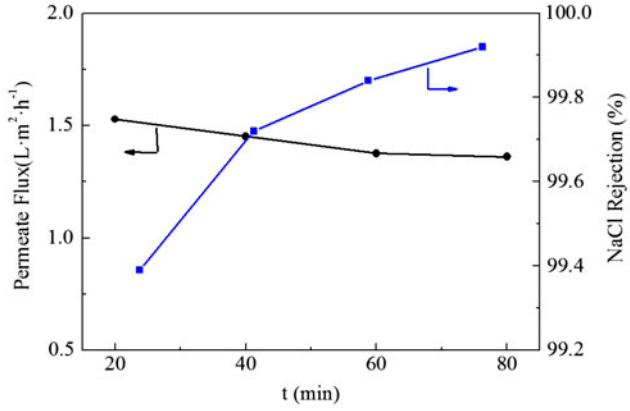

Fig. 14. Permeate flux and NaCl rejection of FEP flat-sheet membranes as 60 wt% DOP content (Feed temperature, 70˚C; Vacuum pressure, −0.09 Mpa; NaCl concentration, 35 g L^{-1}).

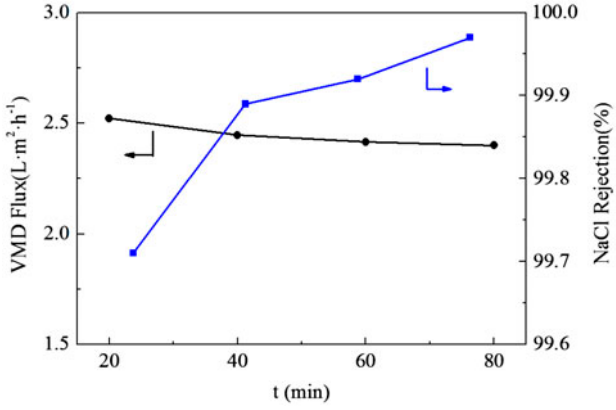

Fig. 15. Permeate flux and NaCl rejection of FEP flat-sheet membranes as 8 wt% SiO_2 content (Feed temperature, 70˚C; Vacuum pressure, −0.09 Mpa; NaCl concentration, 35 g L^{-1}).

3.5. Membrane distillation performance

The FEP membranes with 60% DOP and 8% SiO_2 were tested for the VMD process to evaluate the MD application. In VMD process, the feed temperature was heated to 70˚C, NaCl concentration (35 g L^{-1}), and the vacuum pressure was added to − 0.09 MPa. The MD permeation flux and NaCl rejection results were shown in Figs. 14 and 15. It could be seen that the FEP membrane had a low-permeation flux and a high-NaCl rejection. The max rejection reached as high as 99.97% when the SiO_2 content was 8 wt%. Moreover, with the increase in time, it was found that the MD permeation flux reduced while the NaCl rejection improved at the same feeding temperature.

Table 3
Comparison of the maximum flux obtained in this study with the literature for VMD processes

Membrane code	Porosity (%)	Feed solution	Feed temperature (°C)	NaCl rejection (%)	Permeate flux (L m^{-2} h^{-1})	Refs.
PP flat-sheet	75	100 g L^{-1} NaCl	55	–	10.7	[21]
PVDF flat-sheet	79.6	35 g L^{-1} NaCl	80	97.0	11.8	[22]
PTFE flat-sheet	60	35 g L^{-1} NaCl	60	99.0	14.6	[23]
FEP flat-sheet	56	35 g L^{-1} NaCl	70.0	99.9	2.6	This study

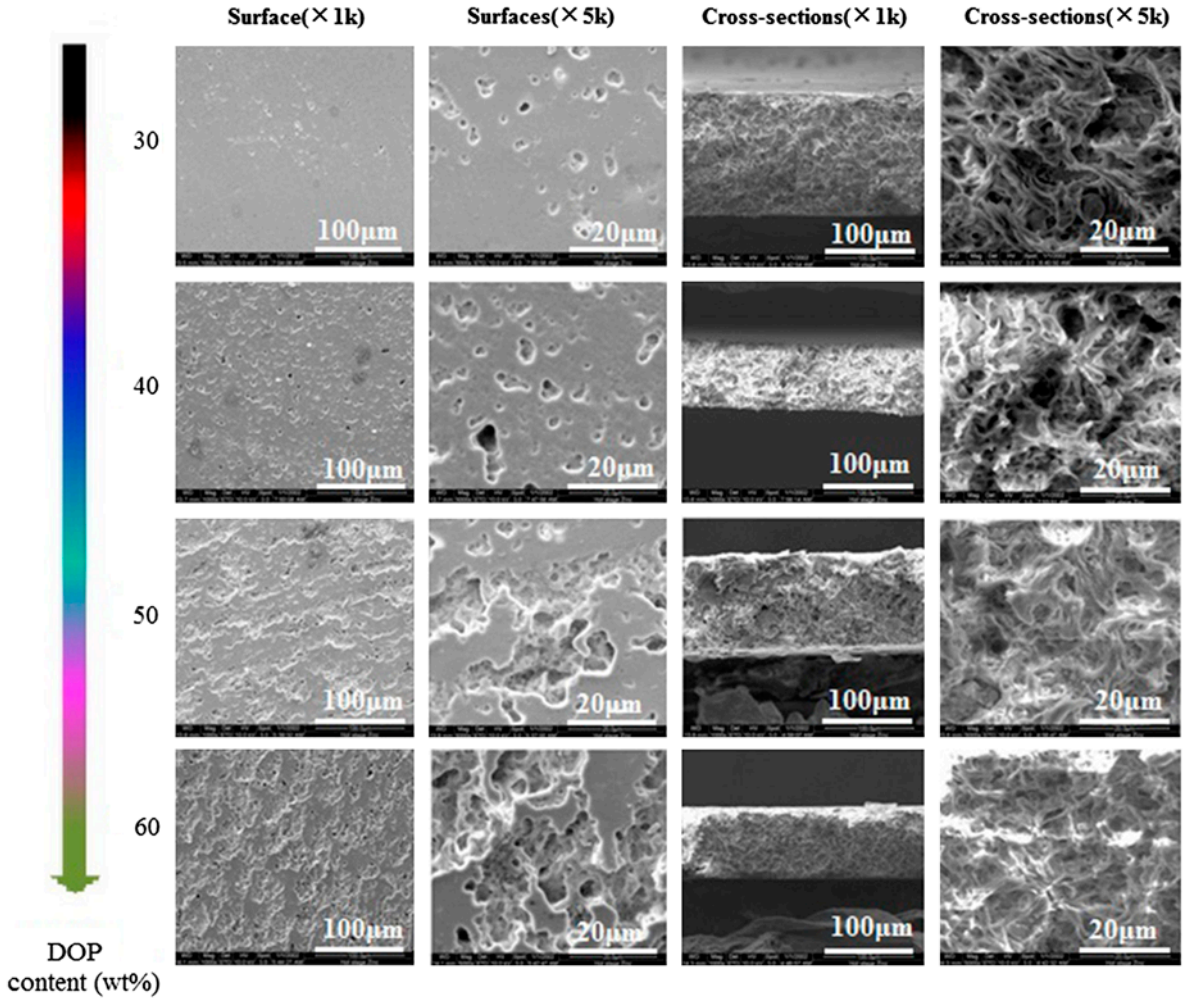

Fig. 16. Morphologies of FEP flat-sheet membranes with different DOP contents.

Table 3 listed a performance comparison between the current work and the previous investigations. It was found that the permeate flux of the FEP blend membrane was lower than other membranes. However, the salt rejection of FEP membrane was the highest.

3.6. Membrane morphology

The surfaces and cross-sections morphologies of FEP flat-sheet membranes were shown in Figs. 16 and 17. It can be seen that the surfaces of FEP flat-sheet membranes exhibited obvious porous structures with

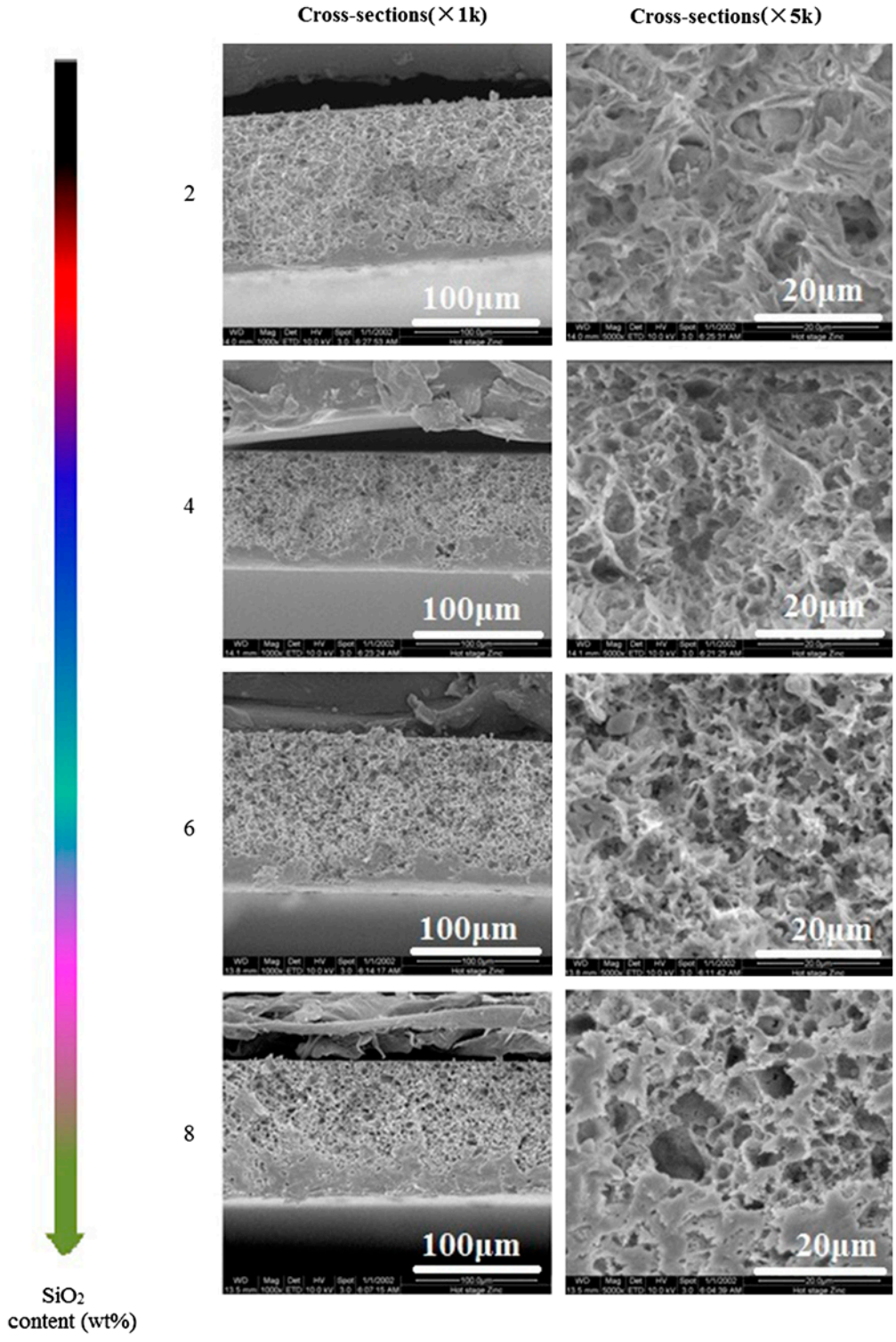

Fig. 17. Cross-sections morphologies of FEP flat-sheet membrane with different SiO_2 contents.

the increase in DOP contents (Fig. 16), and there was no obvious changes in the cross-sections (Fig. 16). Meanwhile, it could be observed that all the membranes displayed a typical asymmetric structure from the morphologies of cross-section. SiO_2 contents played a very important role in the membranes'

cross-section (Fig. 17). As for the cross-section morphologies, it could be seen that the mesh pore structure became larger and deeper with an increase in the SiO_2 contents. The reasons could be concluded that the SiO_2 particles were dissolved.

4. Conclusions

A kind of FEP hybrid flat-sheet membranes were fabricated by melt-compressed membrane formation system which composed of FEP, microscale SiO_2 and DOP. Effects of DOP and SiO_2 contents on the morphology and properties of the FEP membranes were investigated. The increase in DOP and SiO_2 contents brought about an obvious enhancement of PWF and porosity. The pore structure in the membranes' cross-section became larger and deeper with increasing SiO_2 contents. The salt rejections in VMD process achieved as high as 99.9%.

Acknowledgments

This work was supported by the National Natural Science Foundation of China (No. 21404079, 51273147), Tianjin Scientific and Technology Program (No. 12JCZDJC26600).

Symbols

X_c	—	crystallinity value (%)
ΔH	—	melting enthalpy of the mixtures melting (J g^{-1})
ΔH_m	—	enthalpy for a 100% crystalline (J g^{-1})
ε	—	porosity
ρ_f	—	membrane apparent density (kg m^{-3})
ρ_p	—	polymer density (kg m^{-3})
J_l	—	permeation flux (L m^{-2} h^{-1})
V	—	total permeation (L)
A	—	total permeation area (m^2)
t	—	total permeation time (h)
J_g	—	nitrogen flux (m^3 m^{-2} h^{-1})
L	—	nitrogen flow (m^3 h^{-1})
R	—	rejection (%)
C_p	—	concentration of the ink in the feed
C_f	—	concentration of the permeate solution

References

[1] P. Le-Clech, V. Chen, T.A.G. Fane, Fouling in membrane bioreactors used in wastewater treatment, J. Membr. Sci. 284 (2006) 17–53.
[2] D. Wu, M.R. Bird, The fouling and cleaning of ultrafiltration membranes during the filtration of model tea component solutions, J. Food Process Eng. 30(3) (2007) 293–323.
[3] M. Liu, S. Yu, M. Qi, Q. Pan, C. Gao, Impact of manufacture technique on seawater desalination performance of thin-film composite polyamide-urethane reverse osmosis membranes and their spiral wound elements, J. Membr. Sci. 348 (2010) 268–276.
[4] S. Simone, A. Figoli, A. Criscuoli, M.C. Carnevale, A. Rosselli, E. Drioli, Preparation of hollow fiber membranes from PVDF/PVP blends and their application in VMD, J. Membr. Sci. 364 (2010) 219–232.
[5] K.W. Lawson, D.R. Lloyd, Membrane distillation, J. Membr. Sci. 124 (1997) 1–25.
[6] J. Zhang, N. Dow, M. Duke, E. Ostarcevic, S. Gray, Identification of material and physical features of membrane distillation membranes for high performance desalination, J. Membr. Sci. 349 (2010) 295–303.
[7] C.K. Chiam, R. Sarbatly, Heat transfer in the rectangular cross-flow flat-sheet membrane module for vacuum membrane distillation, Chem. Eng. Process. 79 (2014) 23–33.
[8] H. Fan, Y. Peng, Application of PVDF membranes in desalination and comparison of the VMD and DCMD processes, Chem. Eng. Sci. 79 (2012) 94–102.
[9] J. Chen, M. Asano, T. Yamaki, M. Yoshida, Preparation of sulfonated crosslinked PTFE-graft-poly(alkyl vinyl ether) membranes for polymerr electrolyte membrane fuel cells by radiation processing, J. Membr. Sci. 256 (2005) 38–45.
[10] M. Goessi, T. Tervoort, P. Smith, Melt-spun poly(tetrafluoroethylene) fibers, J. Mater. Sci. 42 (2007) 7983–7990.
[11] Z.L. Cui, E. Drioli, Y.M. Lee, Recent progress in fluoropolymers for membranes, Prog. Polym. Sci. 39 (2014) 164–198.
[12] H.L. Zhu, H.J. Wang, F. WangY.H. Guo, H.P. Zhang, Preparation and properties of PTFE hollow fiber membranes for desalination through vacuum membrane distillation, J. Mater. Sci. 446 (2013) 145–153.
[13] T. Imae, Fluorinated polymers, Curr. Opin. Colloid Interface Sci. 8 (2003) 307–314.
[14] Q.L. Huang, C.X. Xiao, X.Y. Hu, A novel method to prepare hydrophobic poly(tetrafluoroethylene) membrane and its properties, J. Mater. Sci. 45 (2010) 6569–6573.
[15] R.A. Morgan, W.H. Tumonello, M.E. Wagman, Low melting tetrafluoroethylene copolymer and its uses, US Pat. 5397829 (1995).
[16] D. Holmes, E. Fasig, Tetrafluoroethylene fine powder resin of a copolymer of tetrafluoroethylene and perfluoro (alkyl vinyl ether), US Pat. 3819594 (1974).
[17] Q.L. Huang, C.F. Xiao, X.Y. Hu, S.L. An, Fabrication and properties of poly(tetrafluoroethylene-co-hexafluoropropylene) hollow fiber membranes, J. Mater. Chem. 21 (2011) 16510–16516.
[18] B. Menzel, T.A. Blanchet, Enhanced wear resistance of gamma-irradiated PTFE and FEP polymers and the

effect of post-irradiation environmental handling, Wear 258 (2005) 935–941.
[19] B.S. Parekh, R.B. Patel, K.S. Cheng, Hollow fiber membrane contact apparatus and process, US Pat. 7717405 (2010).
[20] J.M. Covitch, Method for making a porous fluorinated polymer structure, US Pat. 4434116 (1984).
[21] M. Safavi, T. Mohammadi, High-salinity water desalination using VMD, Chem. Eng. J. 149 (2009) 191–195.
[22] H.W. Fan, Y.L. Peng, Application of PVDF membranes in desalination and comparison of the VMD and DCMD processes, Chem. Eng. Sci. 79 (2012) 94–102.
[23] J.P. Mericq, S. Laborie, C. Cabassud, Vacuum membrane distillation of seawater reverse osmosis brines, Water Res. 44 (2010) 5260–5273.